



# Electrochemical determination of budesonide: a common corticosteroid used to treat respiratory diseases such as COVID-19 and asthma

Katarzyna Jedlińska<sup>1</sup> · Katarzyna Trojanowska<sup>1</sup> · Magdalena Strus<sup>2</sup> · Bogusław Baś<sup>1</sup>

Received: 21 June 2023 / Accepted: 14 August 2023 / Published online: 31 August 2023  
© The Author(s) 2023

## Abstract

The outbreak of the COVID-19 pandemic has adversely affected the most important areas of the modern world. One of the challenges related to counteracting the effects of the pandemic it was necessary to develop methods for the quantitative determination of pharmaceuticals used in the treatment of patients suffering from this disease and its long-term effects. Budesonide (BUD) is a widely available and inexpensive corticosteroid used extensively not only among people suffering from COVID-19, but also asthma and other respiratory diseases. A significant increase in the consumption of drugs containing this component requires the development of new BUD determination methods, especially in real samples. This paper presents a new voltammetric method for BUD determination at renewable silver amalgam film electrode (Hg(Ag)FE). The electrochemical measurements were conducted in the supporting electrolyte containing 80% of methyl alcohol, 0.04 mol L<sup>-1</sup> Britton–Robinson buffer (pH 3.0) and 20 mg mL<sup>-1</sup> of NaClO<sub>4</sub> under optimized differential pulse voltammetry (DPV) parameters. Detailed studies of the behaviour of the BUD on the surface of Hg(Ag)FE demonstrated the quasi-irreversible nature of the diffusion-controlled, two electrons and two protons reduction process. A calibration curve in the range from 1.0 to 290 µg mL<sup>-1</sup> shows limit of detection and limit of quantification equal to 0.06 and 0.21 µg mL<sup>-1</sup>, respectively. The impact of numerous interferences over a wide range of concentrations on BUD signals was analysed and evaluated. The utility of the proposed method was verified by the quantitative analysis of BUD in two pharmaceutical products and the spiked water samples.

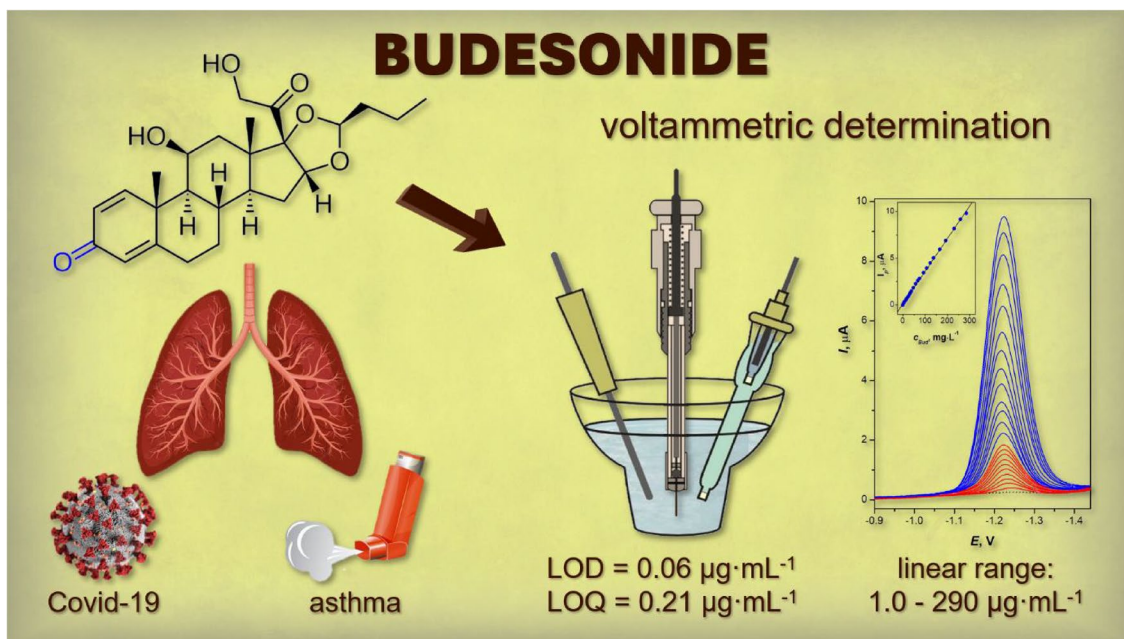
---

✉ Katarzyna Jedlińska  
jedlinska@agh.edu.pl

<sup>1</sup> Faculty of Materials Science and Ceramics, AGH University of Krakow, Mickiewicza 30, 30-059 Krakow, Poland

<sup>2</sup> Chair of Microbiology, Jagiellonian University Medical College, Czysta 18, 31-121 Krakow, Poland

## Graphical abstract



**Keywords** COVID-19 · Budesonide · Respiratory diseases · Voltammetry · Pharmaceuticals

## 1 Introduction

The COVID-19 disease caused by severe acute respiratory syndrome coronavirus 2 (SARS-CoV-2) has become one of the major global public health threats in recent years. We are currently struggling with the long-term effects of the pandemic with a wide range of impacts: health, environmental, social, economic, psychological and even political [1–6]. One of the issues that has arisen was the problem of environmental pollution with pharmacological agents, widely used during treatment of COVID-19 patients, which implied the need to search for new, highly sensitive methods of their determination [6].

BUD is available as a nasal spray, oral delayed-release capsules, inhalation or nebulization suspension and suppositories [7, 8]. It belongs to a corticosteroid-type medications. The chemical name of this substance is 22(R,S)-16 $\alpha$ ,17 $\alpha$ -butylidenedioxy-11 $\beta$ ,21-dihydroxypregna-1,4-diene-3,20-dione. BUD molecule is a mixture of R and S diastereomers, the former of which is characterized by 2–3 times greater topical glucocorticoid potency [9].

Budesonide (BUD) is synthetic corticosteroid present in various pharmaceuticals whose effectiveness in the treatment of COVID-19, especially at the early stage of the disease, has been confirmed by numerous studies [10–12]. BUD has a very strong local anti-allergic and anti-inflammatory effect, it has been commercially available since the 1980s and it has

been commonly used in asthma [13], chronic obstructive pulmonary disease [14, 15] rhinitis [16] and Crohn's disease treatment [7]. Many drugs containing BUD as an active ingredient have already gone through all the stages of drug development process, pharmaceutical legislation and its short- and long-term side effects were well-known. Therefore, during the COVID-19 pandemic they were frequently prescribed by doctors and their use increased significantly. For this reason, it is extremely important to develop new and improve existing procedures for BUD determination.

BUD has so far been determined by different analytical methods, mainly by high-performance liquid chromatography (HPLC) tandem with radioimmunoassay HPLC/RIA [17], and HPLC–UV [18, 19], A reversed-phase ultra-fast liquid chromatography (RP-UFLC) [20] and dispersive liquid–liquid microextraction based on solidification of floating organic droplet DLLME–SFO–HPLC–UV [21] methods as well as liquid chromatography-tandem mass spectrometry (LC–MS/MS) [22] were used to determine this substance. Other methods used to determine this compound were UV–Vis spectrophotometry [23] and square wave-adsorptive stripping voltammetry (SW AdSV) [24]. Microemulsion electrokinetic chromatography (MEEKC), which is a capillary electrophoresis (CE) technique, was used for BUD separation [25]. According to the literature BUD.

The purpose of this paper was to develop and validate a novel voltammetric method for BUD determination. All

experiments were performed using a renewable silver amalgam film electrode (Hg(Ag)FE) [26, 27] which was characterized by excellent parameters, such as excellent repeatability, reproducibility and long-term stability (a few thousand measurement cycles) of the electrode as well as high sensitivity and good linearity of measurements. The Hg(Ag)FE has been successfully applied in quantitative analysis of numerous compounds [28–31]. Since the BUD molecule, similarly to the vitamin K<sub>2</sub> molecule, contains a distinctive quinone ring, in the early stages of the research, we relied on the previously developed method of voltammetric determining vitamin K<sub>2</sub> [32–34]. Developed procedure was thoroughly optimized and the mechanism of the BUD reduction reaction on the Hg(Ag)FE surface was investigated. Selectivity of the presented procedure was verified by examining the influence of several substances that usually appear in pharmaceutical, environmental and biological samples. The practical usefulness of the method was confirmed by pharmaceutical formulation and CRMs analysis.

## 2 Experimental

### 2.1 Apparatus

Voltammetric experiments were performed by means of the M161 electrochemical analyser in combination with the M164 electrode stand (both MTM-Anko, Poland) equipped with a magnetic stirrer. The voltammetric data were measured with accuracy of  $\pm 0.1$  nA for current and  $\pm 1$  mV for potential and processed using EAPro software. The measurements were conducted in conventional glass voltammetric cell equipped with a three-electrode system mode, consists of: renewable silver amalgam film electrode (Hg(Ag)FE, MTM-Anko, Poland) with a surface of  $0.06\text{ cm}^2$ , renewed before each measurement as a working electrode; the silver chloride double-junction Ag|AgCl|3 M KCl|2.5 M KNO<sub>3</sub> as a reference electrode and the Pt wire as an counter electrode. All potentials were referred to the reference electrode described above. All solutions used for analyses were purged with argon.

### 2.2 Reagents

All chemicals were of analytical grade and used as received without further purification. The aqueous solutions were prepared with the bi-distilled water. All experiments were carried out at room temperature.

The BUD standard stock solution ( $1000\text{ }\mu\text{g}\text{-mL}^{-1}$ ) was prepared weekly by dissolving of an appropriate amount of budesonide (Sigma-Aldrich, USA) in methanol (POCH, Poland) and stored in fridge. All diluted solutions of BUD

were prepared shortly before the measurements from the stock solution.

Boric acid, phosphoric acid, acetic acid, sodium hydroxide, citric acid, sodium citrate and disodium phosphate were purchased from POCH (Poland) and sodium acetate was obtained from Sigma-Aldrich (USA). The Britton-Robinson buffer solutions ( $0.04\text{ mol L}^{-1}$ , pH 2.0–11.0) were prepared by mixing appropriate volumes of  $0.04\text{ mol L}^{-1}$  mixture of boric acid, acetate acid and phosphoric acid with  $0.2\text{ mol L}^{-1}$  sodium hydroxide solution. The acetate buffer solutions ( $0.1\text{ mol L}^{-1}$ , pH 3.5–6.2) were prepared from acetic acid sodium acetate solutions. The citrate buffer solutions ( $0.1\text{ mol L}^{-1}$ , pH 3.0–6.0) were prepared from citric acid and sodium citrate solutions. The citrate-phosphate buffer solution ( $0.2\text{ mol L}^{-1}$ , pH 3.5) were obtained by mixing appropriate amount of citric acid and disodium phosphate solutions. Other tested solvents and components of the supporting electrolyte, i.e., methanol, ethanol were obtained from POCH (Poland) and 2-propanol, NaClO<sub>4</sub> and LiClO<sub>4</sub> were obtained from Sigma-Aldrich (USA).

For interference studies sodium dodecyl sulphate (SDS), Triton X-100, hexadecyltrimethylammonium bromide (CTAB), titanium dioxide, uric acid, lactose, magnesium sulphate, magnesium stearate (all from Sigma-Aldrich, USA) as well as starch, calcium carbonate, glucose, ascorbic acid obtained (from POCH, Poland) were used.

The Certified Reference Materials of Surface Water SPS-SW1 Batch no. 114 and Waste Water SPS-WW1 Batch no. 114 from Spectrapure Standards AS (Norway) were used to confirm the usefulness of presented method for analysis of BUD in samples with complex matrix.

### 2.3 Standard procedures

Unless otherwise noted all measurements were carried out in the supporting electrolyte containing 80% of methyl alcohol,  $0.04\text{ mol L}^{-1}$  Britton-Robinson buffer (pH 3.0) and  $20\text{ mg mL}^{-1}$  of NaClO<sub>4</sub> with total volume of 5 mL. The solution was deoxygenated with argon for 3 min before the measurements as well as during the measurements. The surface of the working electrode (Hg(Ag)FE) was refreshed before each measurement in accordance with the procedure described in detail in [26, 27]. For each experiment, at least two independent assays were carried out. Each analytical evaluation was repeated three times.

The electrochemical behaviour of BUD ( $9.9\text{ }\mu\text{g mL}^{-1}$ ) was studied based on the cyclic voltammograms (CVs) recorded for the scan rates ( $\nu$ ) from  $0.00625$  to  $1.00\text{ V s}^{-1}$  in the potential range from  $-0.90$  to  $-1.45\text{ V}$ .

Quantitative determination of BUD concentration was performed using differential pulse voltammetry (DPV) and standard addition method. The DP voltammograms were recorded in the potential range from  $-0.9$  to  $-1.45\text{ V}$ , using

the step potential  $E_s = 3$  mV, pulse amplitude  $dE = 30$  mV, waiting time  $t_w = 5$  ms and the current sampling time  $t_s = 5$  ms.

## 2.4 Real samples preparation procedure

Pharmaceutical formulation Miflonide Breezhaler (Novartis Poland) in the form of powder for inhalation in capsules, containing 200  $\mu\text{g}$  of budesonide per inhalation dose was purchased from local pharmacy. For the analysis of BUD, the content of 1 capsule was dissolved in methanol in 5 mL volumetric flask and sonicated for 5 min the fully dissolved solution was ready for further analysis. The second study drug was Nebbud (Teva Pharmaceuticals Poland), a nebulizable suspension containing 250  $\mu\text{g}$  in 1 mL of the product, which was also obtained from local pharmacy. This drug did not require any preparatory procedure.

For quantitative determination of budesonide in the above-mentioned pharmaceuticals, 50  $\mu\text{L}$  of the analysed solution was transferred to 5 mL of the supporting electrolyte. The DPV measurements were conducted according to parameters described in Sect. 2.3 and the standard addition method included the registration of signals for blank and after the introduction of the sample and subsequent additions of the budesonide standard solution. Recoveries were calculated in sample solution spiked with 100 and 200  $\mu\text{g mL}^{-1}$  of BUD.

Since tap water nor the CRMs of surface and waste water did not contain budesonide, it was spiked with BUD standard solution to obtain concentrations of 50.00 and 100.0  $\mu\text{g mL}^{-1}$ . Samples prepared in this way were analysed in accordance with previously described procedure for the determination of the analyte in pharmaceuticals.

## 3 Results and discussion

### 3.1 Voltammetric behaviour of budesonide on hg(Ag)FE

In order to provide the comprehensive information about the reversibility nature of the red-ox reaction of BUD at the Hg(Ag)FE surface (adsorption-controlled or diffusion-controlled) as well as the mass transport in diffusion layer the CV technique was employed. The effect of scan rate ( $\nu$ ) in the range from 0.006 to 1.00  $\text{V s}^{-1}$  on BUD (9.9  $\mu\text{g mL}^{-1}$ ) peak current ( $I_p$ ) and peak potential ( $E_p$ ) was analysed. CV measurements (Fig. 1a) revealed the presence of a clearly outlined cathode peak at the potential close to  $-1.2$  V and a very small, difficult to analyse anode peak what may indicate the quasi-irreversible character of the electrode reaction.

Analysis of the obtained data, the particularly linear relationship between square root of the scan rate ( $\nu^{1/2}$ ) and the value cathodic peak current ( $I_p$ ) indicates the diffusive nature

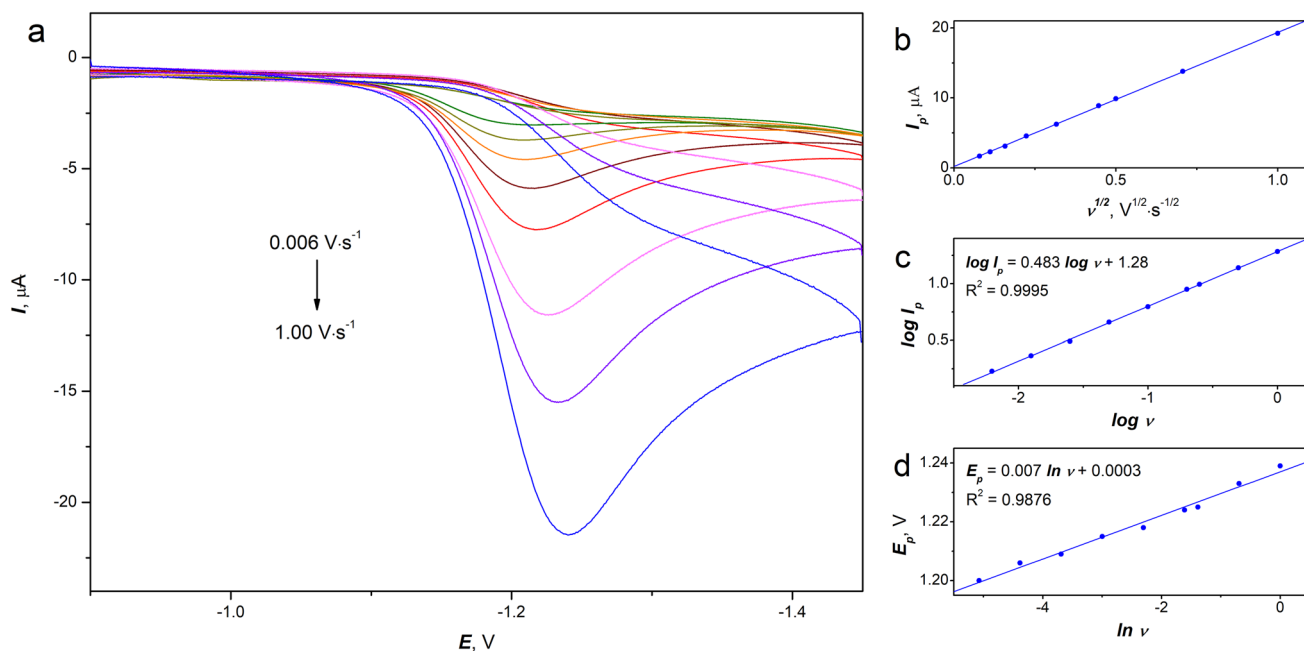


**Fig. 1** Cyclic voltammograms of BUD (9.9  $\mu\text{g mL}^{-1}$ ) at the Hg(Ag) FE in the supporting electrolyte containing 80% of methyl alcohol, 0.04 mol L<sup>-1</sup> Britton–Robinson buffer (pH 3.0) and 20 mg mL<sup>-1</sup> of NaClO<sub>4</sub> in the potential range from  $-0.90$  to  $-1.45$  V, recorded for increasing scan rate values in the range of 0.006–1.00  $\text{V s}^{-1}$ . **A** Cyclic

voltammograms. **B** The dependence of the peak current ( $I_p$ ) on the square root of scan rate ( $\nu^{1/2}$ ). **C** The dependence of logarithm of the peak current ( $\log I_p$ ) on logarithm of scan rate ( $\log \nu$ ). **D** The dependence of the peak potential ( $E_p$ ) on natural logarithm of scan rate ( $\ln \nu$ )

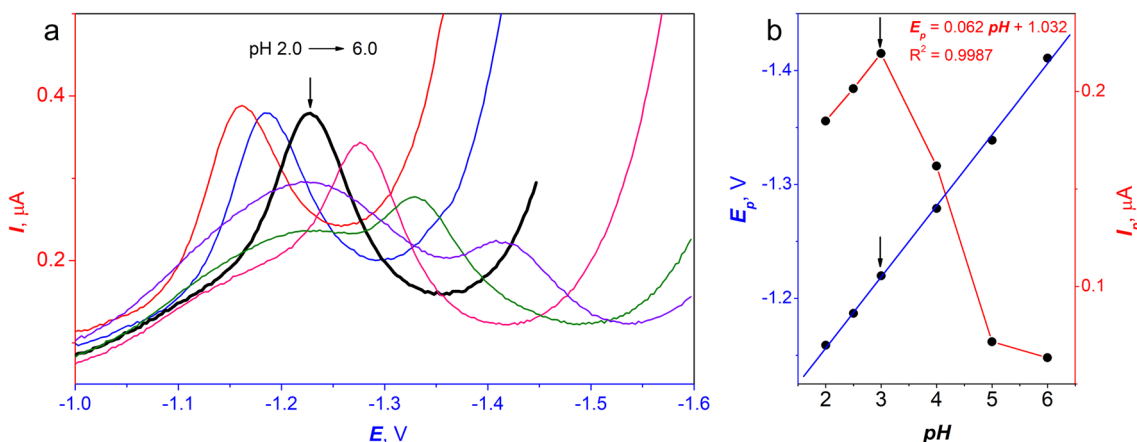


**Fig. 2** Effects of pH values of Britton–Robinson buffer on signals for  $5 \mu\text{g mL}^{-1}$  of BUD. **a** Registered voltammograms. **b** Dependence of peak potential ( $E_p$ , blue line) and current ( $I_p$ , red line) on pH. Arrows

show results for pH of 3.0, which was chosen for subsequent experiments. Other parameters as in Sect. 2.3. (Color figure online)

of the electrode process taking place on the Hg(Ag)FE surface (Fig. 1b). This was also confirmed by the linear dependence of the logarithm of the peak current ( $\log I_p$ ) upon the logarithm of the scan rate ( $\log \nu$ ) (Fig. 1c). The calculated slope of 0.48 was very close to the theoretically expected slope value of 0.50 characterizing diffusion-controlled processes. Furthermore, as the value of the scan rate increased, the peak potential shifted towards the more negative potentials. The dependence of  $E_p$  in function of  $\ln \nu$  shows a linear dependence with the slope equal to 0.007 (Fig. 1d).

Further studies were aimed at confirming the mechanism of the redox reaction using the DPV technique. In accordance with the procedure described in Sect. 2.3. the effect of different pH values (in the range of 2.0–6.0) of the Britton–Robinson buffer on  $5 \mu\text{g mL}^{-1}$  of BUD was investigated. Analysis of the recorded signals (Fig. 2) clearly indicates that the BUD peak current ( $I_p$ ) and potential ( $E_p$ ) strongly depend on the supporting electrolyte pH value. With increasing pH value  $E_p$  was shifting toward more positive potentials. This relationship was characterized by a strong linearity with a slope of  $0.062 \text{ V pH}^{-1}$ , which was close to the theoretical value from the Nernst equation of  $0.059 \text{ V pH}^{-1}$ . This result indicates the transfer of equal number of protons and electrons during the electrochemical reaction of BUD on the surface of the Hg(Ag)FE. It should also be noted that for higher pH values of 5 and 6 the voltammograms show a wide signal with a maximum at a potential of about  $-1.23 \text{ V}$ . This wave was visible in the supporting electrolyte, without the addition of BUD and may be the reason for the attenuation of the BUD signal.

The recorded DPV curves show the presence of the BUD peaks in both cathodic and anodic scans. A large disproportion in recorded peak heights can be noticed – the cathodic peak was 4.5 times higher than the anodic peak. It was also

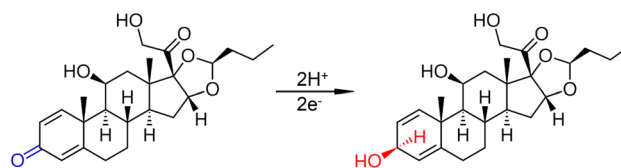


**Fig. 3** Possible electrochemical reduction mechanism of budesonide on Hg(Ag)FE

characterized by greater stability, smaller half-width and a more favourable signal to background ratio. Therefore, in further experiments, only the cathodic signals of BUD reduction were recorded and analysed. The potential difference between the peak maxima ( $E_{pa} - E_{pk} = 0.025 \text{ V}$ ) was 2.2 times smaller than the theoretical value of  $0.057 \text{ V}$ , what suggest that the number of the electrons exchanged in the BUD electrochemical reaction was 2.

Considering all obtained results, it can be assumed that electrochemical reaction of BUD on the surface of Hg(Ag)FE was a quasi-reversible process controlled by diffusion with two electrons and two protons transfer. The registered electrochemical signals may arise as a result of the reduction reaction of the carbonyl functional group to the hydroxyl functional group (Fig. 3). These conclusions were in line with data reported previously in the literature [24, 35].

### 3.2 Composition of supporting electrolyte

The composition of supporting electrolyte strongly affects BUD peak current and potential, therefore the effect of each component on BUD ( $5 \mu\text{g mL}^{-1}$ ) peak current was thoroughly examined.

Since in voltammetric experiments the analyte needs to be completely soluble and BUD is practically insoluble in

water [36] the presence of non-polar solvent is necessary for its proper dissolution in supporting electrolyte. Hence, the influence of methanol content (in the range from 20 to 90%) was studied in acetate buffer (pH 3.8) and 20 mg mL<sup>-1</sup> of NaClO<sub>4</sub>. Low concentration of alcohol results in recording unrepeatable signals with asymmetric peaks. With increasing methanol content, the height of the recorded peak current initially decreases and then systematically increases. The effect of NaClO<sub>4</sub> concentration in the range from 0 to 30 mg mL<sup>-1</sup> on the BUD signal was also tested. The content of 80% methanol and 20 mg mL<sup>-1</sup> of NaClO<sub>4</sub> was found to be optimal for voltammetric BUD determination. Thus, these concentrations were used in all further experiments conducted also with other buffers. It was also verified that replacing methanol with ethanol and 2-propanol results in a reduction of the signal by 55% and 85%, respectively, and replacing NaClO<sub>4</sub> with LiClO<sub>4</sub> results in a reduction of the signal by 10%.

In the next step, the current responses of the 5 µg mL<sup>-1</sup> of BUD were examined in thirteen different buffer solution with different pH values: acetate buffer (pH 3.5, 3.8, 4.5 and 6.2), citrate buffer (pH 3.0, 4.5, 6.0), citrate-phosphate buffer (pH 3.5) and Britton-Robinson buffer (pH 2.0, 2.5, 3.0, 4.0, 5.0 and 6.0). Conducted studies have shown that pH of the supporting electrolyte has an impact on the BUD peak current and potential. For each tested buffer, the highest peak height was obtained at pH 3.0 or 3.5. Moreover, in each case, the potential of the peak decreased linearly with the increase in pH. Based on the obtained peak height, signal to background ratio and the repeatability of the registered signals the Britton-Robinson buffer of pH 3.0 was selected for further experiments.

### 3.3 DPV parameters

To achieve the best sensitivity of developed electroanalytical procedure, the influence of crucial parameters of DPV technique on peak current of 5 µg mL<sup>-1</sup> BUD was tested. The following instrumental parameters were examined: step potential ( $E_s$ , from 1 to 5 mV), pulse amplitude ( $dE$ , from -70 to -10 mV and from 10 to 70 mV), waiting time and sampling time ( $t_w = t_s$ , from 5 to 30 ms) as well as initial potential ( $E_0$ , from -0.2 to -1.0 V). The optimal parameters were selected based on registered peak height, half-width, signal to background ratio and repeatability of the obtained signals. The best results that met these criteria were obtained with values as follow:  $E_s = 3$  mV,  $dE = 30$  mV,  $t_w = t_s = 5$  ms,  $E_0 = -0.9$  V.

### 3.4 Calibration curve parameters

Under conditions deemed optimal, DPV curves were recorded using the standard addition method in solutions

containing increasing concentrations of BUD in the range from “blank” to 290 µg mL<sup>-1</sup>. Well-shaped, reproducible peaks were obtained, with a maximum at -1.22 V.

Averaged from three measurements, the voltammograms obtained for the blank solution and 33 consecutive additions of the BUD standard are shown in Fig. 4. From each averaged curve, a trend line generated according to a third-degree polynomial was subtracted (Fig. 4b) and then a calibration curve was prepared.

Based on the calculated parameters of the calibration curve, it can be concluded that the sensitivity of the method was  $34.9 \pm 0.2$  nA/(µg mL<sup>-1</sup>). The linearity range of the method was from 1.0 to 290 µg mL<sup>-1</sup> of BUD, and the correlation coefficient  $r$  was 0.9996. The limit of detection (LOD) and limit of quantification (LOQ) calculated as:  $LOD = 3SD/b$  and  $LOQ = 10 SD/b$ , (where  $SD$  was a standard deviation of intercept ( $n=5$ ), and  $b$  stands for the slope of the calibration curve) were estimated as: 0.06 and 0.20 µg mL<sup>-1</sup>, respectively. The measurement precision specifies as the relative standard deviation (RSD) for 5 and 10 µg mL<sup>-1</sup> of BUD ( $n=7$ ) was 3.5 and 4.8%, respectively.

The obtained results were compared with the parameters obtained by means of previously described in the literature analytical methods and summarized in Table 1. As can be seen, there were only a few methods for the determination of this compound among which the developed procedure was characterized by the widest linear range and satisfactory LOD value. It needs to be highlighted that the presented method was in line with the GAC recommendations [37], reducing the need to use harmful reagents. Another significant advantage of the proposed method was the simplicity and speed of the conducted measurements. Recording a single curve, including the time needed to refresh the electrode surface and saving the recorded signal, takes an average of merely 15 s. Therefore, it takes only a few minutes to conduct a full analysis.

### 3.5 Interference study

Considering the possibility of using the developed method for the analysis of real samples (pharmaceutical products and surface and waste water samples), an interference study was carried out. The influence of the following substances was examined: Triton-X100 (non-ionic surfactant), cetrimum bromide (CTAB; cationic surfactant), sodium dodecyl sulphate (SDS; anionic surfactant), magnesium stearate, starch, titanium dioxide, glucose, lactose, uric acid, ascorbic acid and inorganic ions (Na<sup>+</sup>, K<sup>+</sup>, Mg<sup>2+</sup>, Ca<sup>2+</sup>, Cu<sup>2+</sup>, NO<sub>2</sub><sup>-</sup>, NO<sub>3</sub><sup>-</sup>, SO<sub>4</sub><sup>2-</sup>, CO<sub>3</sub><sup>2-</sup>). For each studied interferent (in concentration between 0.2 and 2000 µmol L<sup>-1</sup>) a percentage differences between peak current recorded for 20 µmol L<sup>-1</sup> (8.61 µg·mL<sup>-1</sup>) of BUD measured without and in the

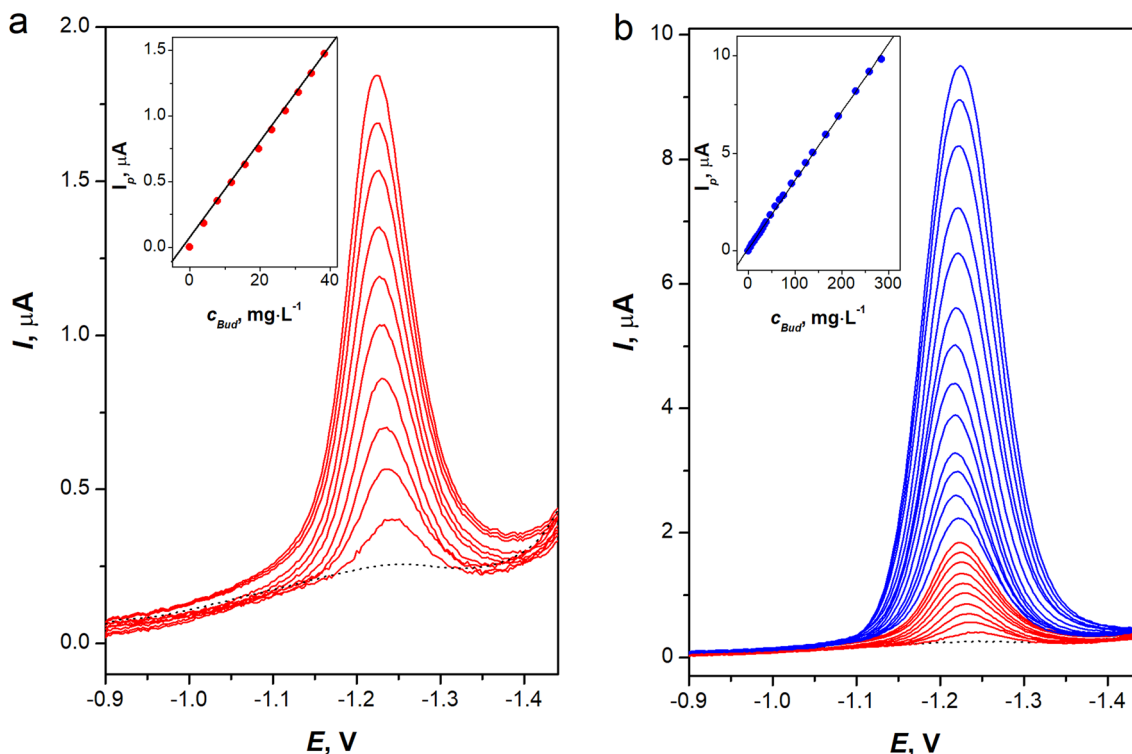


**Fig. 4** DP voltammograms registered at the Hg(Ag)FE achieved for increasing concentrations of BUD in the supporting electrolyte. Concentration of BUD **A** from blank (dotted line) to 38.0  $\mu\text{g mL}^{-1}$  (red

lines), **B** from blank (dotted line) to 290.0  $\mu\text{g mL}^{-1}$  (red and blue lines). Inset: the corresponding calibration plot. Other parameters as in Sect. 2.3. (Color figure online)

**Table 1** Comparison of analytical methods for the determination of BUD

Method	LOD	LOQ	Linear range	Reference
RP-UFLC	2.913 $\mu\text{g mL}^{-1}$	8.76 $\mu\text{g mL}^{-1}$	10–100 $\mu\text{g mL}^{-1}$	[20]
HPLC	0.011 $\mu\text{g mL}^{-1}$	0.035 $\mu\text{g mL}^{-1}$	0.022–8.611 $\mu\text{g mL}^{-1}$	[21]
LC-MS/MS	0.05 $\text{ng mL}^{-1}$	0.1 $\text{ng mL}^{-1}$	0.75–50 $\text{ng mL}^{-1}$	[22]
UV-VIS	0.66 $\mu\text{g mL}^{-1}$	2.019 $\mu\text{g mL}^{-1}$	1.0–25 $\mu\text{g mL}^{-1}$	[23]
SW AdSV	0.040 $\mu\text{mol L}^{-1}$ (0.017 $\mu\text{g mL}^{-1}$ )	0.134 $\mu\text{mol L}^{-1}$ (0.058 $\mu\text{g mL}^{-1}$ )	2–25 $\mu\text{mol L}^{-1}$ (0.9–10.8 $\mu\text{g mL}^{-1}$ )	[24]
DPV	0.06 $\mu\text{g mL}^{-1}$	0.20 $\mu\text{g mL}^{-1}$	1–290 $\mu\text{g mL}^{-1}$	Present work

RP-UFLC reversed-phase ultra-fast liquid chromatography, HPLC high-performance liquid chromatography, LC-MS/MS - liquid chromatography-tandem mass spectrometry, UV-VIS - Ultraviolet-visible spectroscopy, SW AdSV square wave-adsorptive stripping voltammetry, DPV differential pulse voltammetry

presence of interferent were calculated (Fig. 5). The tolerance limit was set as a change less than  $\pm 5\%$ .

None of the tested compounds affected the BUD signal at 0.2 and 2  $\mu\text{mol L}^{-1}$ . Most of studied compounds (SDS, Triton-X100, starch, titanium dioxide, lactose, uric acid and ions:  $\text{K}^+$ ,  $\text{Ca}^{2+}$ ,  $\text{NO}_3^-$ ,  $\text{CO}_3^{2-}$ ) regardless of its concentration, did not influence meaningly the measured signal of BUD. Only the presence of  $\text{Mg}^{2+}$ ,  $\text{Cu}^{2+}$ ,  $\text{SO}_4^{2-}$ ,  $\text{CO}_3^{2-}$  ions at concentration of 2000  $\mu\text{mol L}^{-1}$  and magnesium stearate at 20 and 200  $\mu\text{mol}\cdot\text{L}^{-1}$  resulted in a significant increase of the measured peak current. High concentrations (200 and 2000  $\mu\text{mol L}^{-1}$ ) of glucose, ascorbic acid, CTAB and

magnesium stearate resulted in signal reduction from 9% up to even 28%.

The obtained results indicate that the developed procedure was characterized by high selectivity and can be applied for BUD determination in pharmaceuticals and water samples without complicated sample pretreatment. The possible interference risk occurs only at very high concentrations of interferers (interferent to analyte ratio 10:1 and 100:1). Nevertheless, the risk of distorting the measurement results due to the influence of interfering agents can be compensated by application of sufficient calibration procedure, e.g., the standard addition method

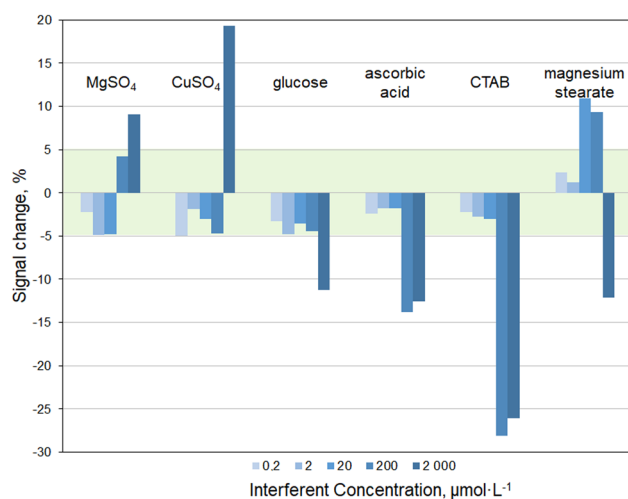


**Fig. 5** Histograms of the signal change of  $20 \mu\text{mol L}^{-1}$  ( $8.61 \mu\text{g mL}^{-1}$ ) of BUD in the presence of interfering agents of various concentrations. Interferents not present in the plot met the criterion of tolerance limit with a signal change less than  $\pm 5\%$

or more complicated procedures, like generalized calibration strategy.

### 3.6 Determination of budesonide in pharmaceutical and water samples

Two different commercially available pharmaceuticals containing BUD were analysed: Nebbud ( $250 \mu\text{g mL}^{-1}$  of BUD) and Miflonide Breezhaler ( $200 \text{ mg}$  of BUD per capsule). Measurements were carried out in accordance with the procedure described in Sect. 2.4 and the standard addition method. Results are presented in Table 2 and an exemplary voltammograms are illustrated in Fig. 6. For Nebbud and Miflonide Breezhaler the relative error values were 2.4 and 3.0% while the RSD values were less than 2.4%, indicating good compliance between the obtained results and the values declared by the producers. Moreover, calculated recoveries were in the range 94–105%.

The described method was also successfully applied for analysis of tap water, surface water CRM SPS-SW1 and waste water CRM SPS-WW1 spiked with 50.0 and  $100.0 \mu\text{g mL}^{-1}$ . The BUD concentration was determined by standard additions method. The obtained results (Table 2) were in good agreement with the total BUD content added to the tested CRM sample solution.

Calculated recoveries were satisfactory for each analysed sample. Based on the results obtained, it can be concluded that the presented procedure might be assumed as accurate for real sample analysis of pharmaceutical products, tap water, surface water and waste water.

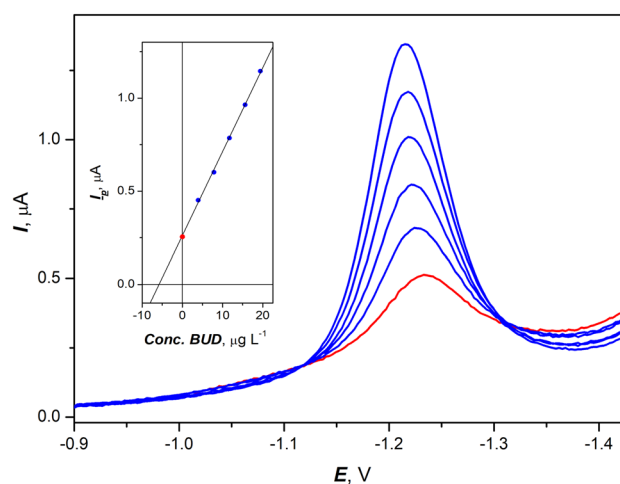


**Fig. 6** An example of standard addition method of DPV determination of BUD in pharmaceuticals material—Nebbud ( $250 \mu\text{g mL}^{-1}$  of BUD) in the supporting electrolyte. Curves: red line: pharmaceutical sample, blue lines: subsequent additions of BUD. Inset: corresponding standard addition plot. Other parameters as in Sect. 2.3. (Color figure online)

## 4 Conclusions

The paper presents a sensitive, precise and accurate voltammetric method for inexpensive and easy determination of BUD by means of differential pulse voltammetry (DPV). As a working electrode a Hg(Ag)FE equipped with a mechanism enabling repeatable and reproducible coating of the surface of silver wire with a thin film of silver amalgam was used successfully.

The procedure of preparing the sensor for electrochemical measurements, as well as the conditions of analyte

**Table 2** Results of BUD determination in pharmaceutical formulation and spiked water samples

Sample	BUD added, $\mu\text{g mL}^{-1}$	BUD determined, $\mu\text{g mL}^{-1}$	Recovery, %
Nebbud ( $250 \mu\text{g mL}^{-1}$ )	0	$256 \pm 2$	–
	100	$358 \pm 4$	104
	200	$461 \pm 5$	105
Miflonide Breezhaler ( $200 \text{ mg}$ per capsule)	0	$194 \pm 4$	–
	100	$286 \pm 5$	95
	200	$377 \pm 6$	94
Tap water	50.00	$49.0 \pm 0.3$	98
	100.0	$103.3 \pm 0.6$	103
Surface water CRM	50.00	$51.5 \pm 0.9$	103
	100.0	$103.8 \pm 1.3$	104
Waste water CRM	50.00	$51.4 \pm 0.5$	103
	100.0	$99.1 \pm 0.8$	99



concentration and instrumental parameters of recording DPV curves, were optimised. Under optimal conditions, the linearity range (1 to 290  $\mu\text{g mL}^{-1}$ ), sensitivity ( $34.9 \pm 0.2 \text{ nA}/(\mu\text{g mL}^{-1})$ ), limit of detection ( $\text{LOD} = 0.06 \mu\text{g mL}^{-1}$ ), limit of quantification ( $\text{LOQ} = 0.20 \mu\text{g mL}^{-1}$ ) and precision of the method (4.8%) were described.

Application of developed procedure allowed for precise and accurate determination of BUD in pharmaceuticals and spiked tap water, surface water and waste water CRM samples without requirement of complicated sample preparation or modification of working electrode surface. Considering obtained results it might be assumed that presented voltammetric method for BUD determination on Hg(Ag) FE was characterized by a wide range of applicability and it stands out from the previously reported work due to its very short time of measurements, simplicity and high sensitivity. Moreover, presented procedure follows the concept of Green Analytical Chemistry, which was in line with the growing requirements for modern analytical methods.

**Author contributions** KJ: Conceptualization, Methodology, Validation, Formal analysis, Investigation, Writing—Original Draft, Writing—Review & Editing, Visualization. KT: Writing—Original Draft. MS: Supervision, Funding acquisition. BB: Conceptualization, Writing—Review & Editing, Supervision, Resources, Funding acquisition.

**Funding** This work was supported by the National Science Centre, Poland (Project No. 2018/31/B/NZ6/02472). Research project partly supported by program “Excellence initiative – research university” for the AGH University of Krakow.

## Declarations

**Competing interest** The authors declare no competing interests.

**Open Access** This article is licensed under a Creative Commons Attribution 4.0 International License, which permits use, sharing, adaptation, distribution and reproduction in any medium or format, as long as you give appropriate credit to the original author(s) and the source, provide a link to the Creative Commons licence, and indicate if changes were made. The images or other third party material in this article are included in the article's Creative Commons licence, unless indicated otherwise in a credit line to the material. If material is not included in the article's Creative Commons licence and your intended use is not permitted by statutory regulation or exceeds the permitted use, you will need to obtain permission directly from the copyright holder. To view a copy of this licence, visit <http://creativecommons.org/licenses/by/4.0/>.

## References

- Chen C, Hauptert SR, Zimmermann L, Shi X, Fritsche LG, Mukherjee B (2022) Global prevalence of post-coronavirus disease 2019 (COVID-19) condition or long COVID: a meta-analysis and systematic review. *J Infect Dis* 226(9):1593–1607. <https://doi.org/10.1093/infdis/jiac136>
- Merad M, Blish CA, Sallusto F, Iwasaki A (2022) The immunology and immunopathology of COVID-19. *Science* 375(6585):1122–1127. <https://doi.org/10.1126/science.abm8108>
- Ceban F, Ling S, Lui LMW, Lee Y, Gill H, Teopiz KM, Rodrigues NB, Subramaniapillai M, Di Vincenzo JD, Cao B, Lin K, Mansur RB, Ho RC, Rosenblat JD, Miskowiak KW, Vinberg M, Maletic V, McIntyre RS (2022) Fatigue and cognitive impairment in post-COVID-19 syndrome: a systematic review and meta-analysis. *BBI Health* 101:93–135. <https://doi.org/10.1016/j.bbi.2021.12.020>
- Bethhäuser BA, Bach-Mortensen AM, Engzell PA (2023) A systematic review and meta-analysis of the evidence on learning during the COVID-19 pandemic. *Nat Hum Behav* 7:375–385. <https://doi.org/10.1038/s41562-022-01506-4>
- Filchakova O, Dossym D, Ilyas A, Kuanysheva T, Abdizhamil A, Bukasov R (2022) Review of COVID-19 testing and diagnostic methods. *Talanta* 244:123409. <https://doi.org/10.1016/j.talanta.2022.123409>
- Robinson PC, Liew DFL, Tanner HL, Grainger JR, Dwek RA, Reisler RB, Steinman L, Feldmann M, Ho LP, Hussell T, Moss P, Richards D, Zitzmann N (2022) COVID-19 therapeutics: challenges and directions for the future. *PNAS* 119(15):e2119893119. <https://doi.org/10.1073/pnas.2119893119>
- López-Sanromán A, Clofent J, Garcia-Planella E, Menchén L, Nos P, Rodríguez-Lago I, Domènech E (2018) Reviewing the therapeutic role of budesonide in Crohn's disease. *Gastroenterol Hepatol* 41(7):458–471. <https://doi.org/10.1016/j.gastre.2018.07.006>
- Ardestani ME, Klantar E, Azimian M (2018) Comparison of the efficacy of budesonide nebulizer suspension and budesonide inhalation suspension in the treatment of acute exacerbation of chronic obstructive pulmonary disease. *Tanaffos* 17(2):96–102
- Matabosch X, Pozo OJ, Pérez-Mañá C, Farré M, Marcos J, Segura J, Ventura R (2012) Identification of budesonide metabolites in human urine after oral administration. *Anal Bioanal Chem* 404(2):325–340. <https://doi.org/10.1007/s00216-012-6037-0>
- Yu LM et al (2021) Inhaled budesonide for COVID-19 in people at high risk of complications in the community in the UK (PRIN-CIPLE): a randomised, controlled, open-label, adaptive platform trial. *The Lancet* 398(10303):843–855. [https://doi.org/10.1016/S0140-6736\(21\)01744-X](https://doi.org/10.1016/S0140-6736(21)01744-X)
- Drożdżał S, Rosik J, Lechowicz K, Machaj F, Szostak B, Przybyciński J, Lorzadeh S, Kotfis K, Ghavami S, Łos MJ (2021) An update on drugs with therapeutic potential for SARS-CoV-2 (COVID-19) treatment. *Rev Drug Resist Updat* 59:100794. <https://doi.org/10.1016/j.drup.2021.100794>
- Lipworth B, Chan R, Misirovs R (2021) High-dose budesonide for early COVID-19. *Lancet* 398(10317):2147. [https://doi.org/10.1016/S0140-6736\(21\)02440-5](https://doi.org/10.1016/S0140-6736(21)02440-5)
- Bateman ED, Hurd SS, Barnes PJ, Bousquet J, Drazen JM, FitzGerald M, Gibson P, Ohta K, O'Byrne P, Pedersen SE, Pizzichini E, Sullivan SD, Wenzel SE, Zar HJ (2008) Global strategy for asthma management and prevention: GINA executive summary. *Eur Respir J* 31:143–178. <https://doi.org/10.1183/09031936.00138707>
- Pauwels RA, Löfdahl C-G, Laitinen LA, Schouten JP, Postma DS, Pride NB, Ohlsson SV (1999) Long-term treatment with inhaled budesonide in persons with mild chronic obstructive pulmonary disease who continue smoking. *N Engl J Med* 340:1948–1953. <https://doi.org/10.1056/NEJM199906243402503>
- Aghili M, Vahidi E, Mohammadrezaei N, Mirrajei T, Abedini A (2020) Effectiveness of nebulized budesonide for COPD exacerbation management in emergency department; a randomized clinical trial. *Arch Acad Emerg Med* 8(1):e85
- Trangsrud AJ, Whitaker AL, Small RE (2002) Intranasal corticosteroids for allergic rhinitis. *Pharmacotherapy* 22(11):1458–1467. <https://doi.org/10.1592/phco.22.16.1458.33692>

17. Hochhaus G, Fröhlich P, Hochhaus R, Möllmann A, Derendorf H, Möllmann HW (1998) A selective HPLC/RIA for the determination of budesonide. *J Pharm Biomed Anal* 17(8):1235–1242. [https://doi.org/10.1016/S0731-7085\(98\)00022-3](https://doi.org/10.1016/S0731-7085(98)00022-3)
18. Demurtas A, Pescina S, Nicoli S, Santi P, Ribeiro de Araujo D, Padula C (2021) Validation of a HPLC-UV method for the quantification of budesonide in skin layers. *J Chromatogr B* 1164:122512. <https://doi.org/10.1016/j.jchromb.2020.122512>
19. Hou S, Hindle M, Byron PR (2001) A stability-indicating HPLC assay method for budesonide. *J Pharm Biomed Anal* 24(3):371–380. [https://doi.org/10.1016/s0731-7085\(00\)00424-6](https://doi.org/10.1016/s0731-7085(00)00424-6)
20. Avuthu Sai S, Mukthinuthalapati Mathrusri A, Rangisetty Spandana Y (2020) New validated stability indicating RP-UFLC method for the determination of budesonide. *Res J Pharm Technol* 13:2819–2824. <https://doi.org/10.5958/0974-360X.2020.00502.8>
21. Hryniewicka M, Starczewska B, Gołębiewska A (2019) Determination of budesonide and sulfasalazine in water and wastewater samples using DLLME-SFO-HPLC-UV method. *Water (Switzerland)* 11(8):1581. <https://doi.org/10.3390/w11081581>
22. Berg S, Melamies M, Rajamäki M, Vainio O, Peltonen K (2012) Liquid chromatography tandem mass spectrometry determination of total budesonide levels in dog plasma after inhalation exposure. *Anal Bioanal Chem* 402(3):1209–1215. <https://doi.org/10.1007/s00216-011-5549-3>
23. Bhusari S, Chaudhari T, Shrangare G, Wakte P (2018) Development and validation of UV-visible spectrophotometric method for estimation of budesonide in bulk And formulation. *J Pharm Res* 7(12):300–304
24. Alghamdi AF (2022) Square wave-adsorptive stripping voltammetric technique development and validation for the determination of budesonide in pharmaceuticals and biological fluids using graphite working electrode. *J Taibah Univ Sci* 16(1):372–380. <https://doi.org/10.1080/16583655.2022.2062883>
25. Altria KD (1999) Application of microemulsion electrokinetic chromatography to the analysis of a wide range of pharmaceuticals and excipients. *J Chromatogr A* 844(1–2):371–386. [https://doi.org/10.1016/S0021-9673\(99\)00350-7](https://doi.org/10.1016/S0021-9673(99)00350-7)
26. Baś B, Kowalski Z (2002) Preparation of silver surface for mercury film electrode of prolonged analytical application. *Electroanalysis* 14(15–16):1067–1071. [https://doi.org/10.1002/1521-4109\(200208\)14:15/16%3c1067::AID-ELAN1067%3e3.0.CO;2-5](https://doi.org/10.1002/1521-4109(200208)14:15/16%3c1067::AID-ELAN1067%3e3.0.CO;2-5)
27. Baś B (2006) Refreshable mercury film silver based electrode for determination of chromium(VI) using catalytic adsorptive stripping voltammetry. *Anal Chim Acta* 570:195–201. <https://doi.org/10.1016/j.aca.2006.04.013>
28. Smarzewska S, Guziejewski D, Leniart A, Ciesielski W (2017) Nanomaterials vs amalgam in electroanalysis: comparative electrochemical studies of lamotrigine. *J Electrochem Soc* 164:B321–B329. <https://doi.org/10.1149/2.0221707jes>
29. Smajdor J, Piech R, Paczosa-Bator B (2018) Highly sensitive voltammetric determination of dexamethasone on amalgam film electrode. *J Electrochem Soc* 89:147–152. <https://doi.org/10.1016/j.jelechem.2017.12.042>
30. Smajdor J, Piech R, Paczosa-Bator B (2018) Spironolactone voltammetric determination on renewable amalgam film electrode. *Steroids* 130:1–6. <https://doi.org/10.1016/j.steroids.2017.12.007>
31. Górska A, Paczosa-Bator B, Piech R (2019) Highly sensitive AdSV Method for Fe(III) determination in presence of solochrome violet RS on renewable amalgam Film electrode. *Electroanalysis* 31(9):1690–1696. <https://doi.org/10.1002/elan.201900204>
32. Jedlińska K, Strus M, Baś B (2018) A new electrochemical sensor with the refreshable silver liquid amalgam film multi-electrode for sensitive voltammetric determination of vitamin K2 (menaquinone). *Electrochim Acta* 265:355–363. <https://doi.org/10.1016/j.electacta.2018.01.204>
33. Jedlińska K, Lipińska J, Smarzewska S, Baś B (2019) The Bi-Disc glassy carbon electrode for determination of vitamin K2 (menaquinone) using stripping voltammetry. *J Electrochem Soc* 166:B360–B366. <https://doi.org/10.1149/2.0331906jes>
34. Smajdor J, Porada R, Lipińska J, Więcek G, Jedlińska K, Baś B, Strus M (2023) Fast and reliable voltammetric determination of menaquinone (vitamin K2) produced in vitro by *Bacillus subtilis* cultures. *J Appl Electrochem*. <https://doi.org/10.1007/s10800-023-01886-z>
35. Morrison RT, Boyd RN (1992) *Organic chemistry*, 6th edn. Prentice Hall, Englewood Cliffs (NJ), pp 425–430
36. O'Neil MJ (ed) (2013) *The merck index - an encyclopedia of chemicals, drugs, and biologicals*. Royal Society of Chemistry, Cambridge, p 259
37. Gałuszka A, Migaszewski Z, Namieśnik J (2013) The 12 principles of green analytical chemistry and the significance mnemonic of green analytical practices. *TrAC Trend Anal Chem* 50:78–84. <https://doi.org/10.1016/j.trac.2013.04.010>

**Publisher's Note** Springer Nature remains neutral with regard to jurisdictional claims in published maps and institutional affiliations.